

Dylan Johnston | 1003852690  
Masters of Engineering  
University of Toronto | UTIAS

---

## Spacecraft Attitude Control Using On-Board Magnetic Dipoles

AER 1503  
Spacecraft Dynamics and Control II  
April 20th, 2018

# Contents

<b>1</b>	<b>Introduction</b>	<b>1</b>
<b>2</b>	<b>Literature Review</b>	<b>1</b>
<b>3</b>	<b>Theory</b>	<b>1</b>
3.1	Background . . . . .	1
3.1.1	Frames of Reference . . . . .	1
3.1.2	Quaternions . . . . .	2
3.1.3	Magnetic Field . . . . .	2
3.2	Dynamics of a Rigid Spacecraft . . . . .	3
3.2.1	Motion of a Rigid Body . . . . .	3
3.3	Magnetic Control of a Rigid Spacecraft . . . . .	3
3.3.1	Passivity . . . . .	3
3.4	Basic Bdot Control . . . . .	3
3.4.1	Detumbling . . . . .	3
3.4.2	Gain . . . . .	4
3.5	Angular Rate feedback . . . . .	4
3.6	State feedback . . . . .	5
3.6.1	Stability . . . . .	5
3.7	Linearized Model . . . . .	5
<b>4</b>	<b>Simulation</b>	<b>7</b>
<b>5</b>	<b>Discussion</b>	<b>11</b>
<b>6</b>	<b>Conclusion</b>	<b>11</b>
<b>7</b>	<b>Matlab Code</b>	<b>13</b>

## List of Figures

1	Comparison of Bdot control and rate feedback control at an altitude of 900km. . . . .	8
2	Comparison of Bdot control and full state feedback control at an altitude of 150km. . . . .	8
3	Comparison of Bdot control law at varying orbital inclinations, at an altitude of 900km . . . . .	9
4	Effect of altitude on time to reach steady state. . . . .	9
5	Bdot control magnetic dipole feedback value during detumble maneuver. . . . .	10
6	Bdot feedback control in near geomagnetic equatorial orbit. . . . .	10

# 1 Introduction

Spacecraft attitude control systems are of paramount importance to the satisfactory achievement and useful longevity of mission objectives. Such control systems are typically comprised of one or more sensors necessary to measure the orientation of the spacecraft, and one or more actuators which are used to orient the craft to some desired attitude. The sensors and actuators are related by a control law which uses the current orientation provided by the sensors, and some predetermined desired orientation, in order to correctly determine the actuation necessary to re-orient the craft.

It is desirable to have a control mechanism which does not require propellant, as on board propellant volume is a firm upper limit on attitude control longevity if the opportunity for refueling is not available. One such technique for attitude control involves the use of electromagnetic coils known as magnetorquers to generate a magnetic field around the spacecraft. This magnetic field interacts with the local ambient magnetic field, typically the Earth's, to generate a useful torque that can be used to control a spacecraft's attitude.

Several challenges face the development of a robust magnetic attitude control system. Magnetic attitude control is most effective in the presence of high flux density magnetic fields; an effective magnetic control system must either be immersed in a strong magnetic field, or must be able to generate large currents within the electromagnetic coils used to generate the magnetic field around the spacecraft. The absence of magnetic fields in deep space render this form of control unsuitable for missions outside a celestial body's magnetosphere. The variability of the Earth's magnetic field based on orbital position renders the magnetic control problem highly non-linear, however several attempts have been made at developing linearized periodic systems due to the periodic nature of orbit. However magnetic torques can only be exerted perpendicularly to a magnetic field, leaving the entire problem underactuated. The problem is further exacerbated if the spacecraft has electrically conductive components, as eddy currents will be generated resulting in unwanted disturbance torques.

This document serves as an investigation into the magnetic control of spacecraft operating in low Earth orbit. Section 2 provides a survey of research papers that have been published on the subject of magnetic attitude control, as well as a general discussion of the various methods that seem most promising. In section 3, a mathematical description of the dynamical system is presented, along with several control laws. The stability of each law is either demonstrated or referenced, since several stability proofs are beyond the scope of this investigation. A matlab simulation was developed using the control laws and dynamics described in section 3, and the results of this simulation are presented in section 4. The results of the simulation are then discussed in section 5.

## 2 Literature Review

Magnetic control of satellites has been of interest since the very onset of the space age. White et al. [16] was one of the first inquiries into the magnetic attitude control problem. The original Bdot control law was proposed in 1976 [12], what has gained traction for use as a detumbling control law. The use of magnetic control in conjunction with gravity gradient stabilized spacecrafts[8] prompted a renewed attempt at a fully magnetic three-axis stability control system[9].

Several strides forward were made in the late 1990's in the development of periodic controllers using Lyapunov stability theory [18] [17] [10] [13]. Recent research has investigated linear quadratic regulator controllers [5] and model predictive controllers [11] [19] in an attempt to fully develop 3-axis magnetic actuation as a form of attitude control.

## 3 Theory

### 3.1 Background

#### 3.1.1 Frames of Reference

**Earth Centered Inertial (ECI)** - The origin of this reference frame lies at the Earth's center, with the positive x-direction determined by the vernal equinox, the positive z-direction aligned with the Earth's north south axis, and the y-direction chosen to complete the right handed triad. This frame will be represented by  $\mathcal{F}_i$ .

**Satellite Orbital Frame** - The origin of this reference frame lies at the center of mass of the rigid spacecraft in question. The positive z-direction is nadir pointing, while the positive x-direction is aligned with the spacecraft's orbital velocity. The positive y-direction lies perpendicular to the orbital plane and is anti-parallel to the spacecraft's orbital angular velocity vector. This frame is represented by  $\mathcal{F}_o$ .

**Principal Body Fixed Frame** - This reference frame is centered on the spacecraft's center of mass, and has the 3 mutually orthogonal axes aligned with the 3 principal axes of the spacecraft. This reference frame is represented using  $\mathcal{F}_b$ .

### 3.1.2 Quaternions

The dynamics of the system is formulated in terms of quaternions. For the most general motion of a rigid body with one point fixed, the rotation matrix about the axis which extends through the fixed point is given by:

$$\mathbf{C} = \cos \phi \mathbf{1} + (1 - \cos \phi) \mathbf{a} \mathbf{a}^T - \sin \phi \mathbf{a}^\times \quad (1)$$

Where  $\phi$  is the rotation about said axis and  $\mathbf{a}$  is the unit normalized vector which points in the direction of the axis. Thus, the attitude of the rigid body can be described by four quantities. When multiple consecutive rotations are considered, an obvious choice of coordinates that could be used to describe the attitude of the spacecraft are given by:

$$\mathbf{q} = \begin{bmatrix} \varepsilon_1 \\ \varepsilon_2 \\ \varepsilon_3 \\ \eta \end{bmatrix}, \quad \boldsymbol{\varepsilon} = \begin{bmatrix} a_1 \sin \frac{\phi}{2} \\ a_2 \sin \frac{\phi}{2} \\ a_3 \sin \frac{\phi}{2} \end{bmatrix} = \mathbf{a} \sin \frac{\phi}{2}, \quad \eta = \cos \frac{\phi}{2} \quad (2)$$

The relationship between angular velocity the rotation matrices,  $\boldsymbol{\omega}^\times = -\dot{\mathbf{C}}\mathbf{C}^T$ , along with equation [1], we arrive at:

$$\boldsymbol{\omega} = \dot{\phi} \mathbf{a} - (1 - \cos \phi) \mathbf{a}^\times \dot{\mathbf{a}} + \sin \phi \dot{\mathbf{a}}$$

This result can be used in conjunction with equations 2 to obtain:

$$\dot{\mathbf{q}} = \frac{1}{2} \begin{bmatrix} 0 & \omega_3 & -\omega_2 & \omega_1 \\ -\omega_3 & 0 & \omega_1 & \omega_2 \\ \omega_2 & -\omega_1 & 0 & \omega_3 \\ -\omega_1 & -\omega_2 & -\omega_3 & 0 \end{bmatrix} \begin{bmatrix} \varepsilon_1 \\ \varepsilon_2 \\ \varepsilon_3 \\ \eta \end{bmatrix} = \frac{1}{2} \begin{bmatrix} -\boldsymbol{\omega}^\times & \boldsymbol{\omega} \\ -\boldsymbol{\omega}^T & 0 \end{bmatrix} \begin{bmatrix} \boldsymbol{\varepsilon} \\ \eta \end{bmatrix} = \frac{1}{2} \mathcal{W}(\boldsymbol{\omega}) \mathbf{q} \quad (3)$$

### 3.1.3 Magnetic Field

The Earth's geomagnetic field is hardly uniform, and varies in value from approximately  $25\mu T$  to  $65\mu T$  at the Earth's surface. A review of the literature has suggested one approximation for the field in terms of a magnetic dipole. The Earth's geomagnetic field can be approximated as a tilted dipole of moment  $M_\oplus = 7.8379 \times 10^6 \text{ T km}^3$ , with a tilt angle of  $\gamma_m = 11.4^\circ$  with respect to the polar axis [15].

Then, for a circular low-Earth orbit of radius  $r_o$ , the components of the geomagnetic vector can be expressed in the orbital frame as [4]:

$$\mathbf{B}_o = \frac{M_\oplus}{r_o^3} \begin{bmatrix} \sin \xi_m \cos (\Omega t - \eta_m) \\ -\cos \xi_m \\ 2 \sin \xi_m \sin (\Omega t - \eta_m) \end{bmatrix}$$

Where:

$$\begin{aligned} \cos \xi_m &= \cos i \cos \gamma_m + \sin i \sin \gamma_m \cos \beta'_m \\ \sin \eta_m \sin \xi_m &= -\sin \gamma_m \sin \beta'_m \\ \cos \eta_m \sin \xi_m &= \sin i \cos \gamma_m - \cos i \sin \gamma_m \cos \beta'_m \\ \beta'_m &= \beta_m + \omega_e t - \Omega_{an} \end{aligned}$$

- $i$  - Orbital inclination with respect to equatorial plane
- $\Omega$  - Orbital rate ( $\Omega = \frac{2\pi}{T}$ )
- $\omega_e$  - Earth's angular rate of rotation
- $\Omega_{an}$  - Ascending node of the spacecraft's orbital plane
- $\beta_m$  - Initial value of the angle between the vernal equinox and the line of intersection of the equatorial plane with the geomagnetic equator
- $\xi_m$  - Inclination of the spacecraft orbit relative to the geomagnetic equatorial plane
- $\eta_m$  - Angle between the ascending node relative to the Earth's equator and the ascending node relative to the geomagnetic equator

The components of the Earth's magnetic field can be expressed in the body fixed frame by using a transformation matrix:

$$\mathbf{B}_b = \mathbf{C}_{bo}\mathbf{B}_o$$

Where the rotation matrix  $\mathbf{C}_{bo}$  is given by:

$$\mathbf{C}_{bo} = (\eta^2 - \boldsymbol{\varepsilon}^T \boldsymbol{\varepsilon})\mathbf{1}_3 + 2\boldsymbol{\varepsilon}\boldsymbol{\varepsilon}^T - 2\eta\boldsymbol{\varepsilon}^\times$$

### 3.2 Dynamics of a Rigid Spacecraft

#### 3.2.1 Motion of a Rigid Body

The components of  $\boldsymbol{\omega}$  are expressed in the body fixed frame,  $\mathcal{F}_b$ . The time evolution of the motion of a rigid spacecraft can be described by Euler's equation:

$$\mathcal{I}\dot{\boldsymbol{\omega}} + \boldsymbol{\omega}^\times \mathcal{I}\boldsymbol{\omega} = \boldsymbol{\tau}$$

Here,  $\mathcal{I}$  is the moment of inertia matrix as expressed in the body fixed frame. The sum of the control torques  $\boldsymbol{\tau}_c$  and disturbance torques  $\boldsymbol{\tau}_d$  are represented by the total torque on the spacecraft,  $\boldsymbol{\tau}$ . Note that disturbance torques are typically comprised of gravity gradient, aerodynamic pressure, solar radiation and magnetic disturbance torques.

### 3.3 Magnetic Control of a Rigid Spacecraft

The control torques are provided by 3 mutually perpendicular dipoles which are oriented on the spacecraft's three principle axes. It is assumed that the spacecraft does not contain any electrically conductive material, and therefore, that no disturbance torques are generated due to eddy current generated magnetic fields. The presence of gravity gradient, aerodynamic, solar radiation and magnetic disturbance torques are ignored. Euler's equation then takes the form:

$$\mathcal{I}\dot{\boldsymbol{\omega}} + \boldsymbol{\omega}^\times \mathcal{I}\boldsymbol{\omega} = \mathbf{m}^\times(t)\mathbf{B}(t) \quad (4)$$

Where  $\mathbf{m}(t)$  is the magnetic dipole moment of the spacecraft, and  $\mathbf{B}(t)$  is the magnetic field vector, both expressed in the body fixed frame.

#### 3.3.1 Passivity

It can be shown that the dynamic system presented above is passive by considering the kinetic energy of the system:

$$\begin{aligned} \mathcal{T} &= \frac{1}{2}\boldsymbol{\omega}^T \mathcal{I}\boldsymbol{\omega} \\ \dot{\mathcal{T}} &= \boldsymbol{\omega}^T \mathcal{I}\dot{\boldsymbol{\omega}} \\ &= \boldsymbol{\omega}^T \left[ -\boldsymbol{\omega}^\times \mathcal{I}\boldsymbol{\omega} - \mathbf{B}(t)^\times \mathbf{m}(t) \right] \\ &= -\boldsymbol{\omega}^T \mathbf{B}(t)^\times \mathbf{m}(t) = \mathbf{m}(t)^T \mathbf{B}(t)^\times \boldsymbol{\omega} \\ \therefore \quad \mathcal{T} &= \int_0^T \mathbf{m}(t)^T \mathbf{B}(t)^\times \boldsymbol{\omega} dt = \mathcal{T}(T) \geq 0 \end{aligned}$$

Where it is assumed that  $T(0) = 0$ . Thus, the dynamic system that has the input  $\mathbf{m}(t)$  and output  $\mathbf{B}^\times \boldsymbol{\omega}$  is passive.

### 3.4 Basic Bdot Control

#### 3.4.1 Detumbling

Based on the passivity argument presented above, a strictly passive negative feedback is suggested:

$$\mathbf{m} = \mathbf{K}\boldsymbol{\omega}^\times \mathbf{B}$$

Rate measurements of  $\boldsymbol{\omega}$  are much more difficult to obtain than measurements of the magnetic field vector at a given instant in time. Noting that the time derivative of the magnetic field vector  $\mathbf{B}$  is given by:

$$\dot{\mathbf{B}} = \overset{\circ}{\mathbf{B}} + \boldsymbol{\omega}^\times \mathbf{B}$$

Where  $\overset{\circ}{\mathbf{B}}(t)$  represents the rate of change of the magnetic field as expressed in the body fixed frame, and  $\dot{\mathbf{B}}(t)$  is due to the spacecraft changing its position in a non-constant magnetic field. If the magnetic field is assumed to be constant ( $\dot{\mathbf{B}}(t) = 0$ ), or the position of the spacecraft to be slowly varying, the standard 'Bdot' control law is obtained:

$$\mathcal{I}\dot{\boldsymbol{\omega}} + \boldsymbol{\omega}^\times \mathcal{I}\boldsymbol{\omega} = -\left(\mathbf{K}\dot{\mathbf{B}}(t)\right)^\times \mathbf{B}(t)$$

Note that the rate of change of the magnetic field can be determined numerically using just measurements of the Earth's magnetic field.

### 3.4.2 Gain

The gain of the detumbling bdot controller is a particularly sensitive control parameter due to the under actuated nature of magnetic dipole control. Since the magnetic dipoles can only generate torque in a direction perpendicular to the local magnetic field, a complete detumbling maneuver requires the local magnetic field to change so that appropriate torques can be applied on all three axes.

Choosing the proper value of the control gain amounts to limiting the gain to be within two extrema: when the gain is high, the transverse component of  $\boldsymbol{\omega}_\perp$  quickly vanishes, and any further reduction of  $\boldsymbol{\omega}$  can only be brought about via changes in the local magnetic field due to changing orbital position. This is not ideal, since  $\boldsymbol{\omega}$  will quickly begin to track the direction of the magnetic field ( $\boldsymbol{\omega} \approx \omega \hat{\mathbf{b}}$ ), and any further dissipation will be quite small. On the other hand, if the gain is set too low, slower dynamics are obviously attained, and the entire detumbling process requires a longer time interval.

In order to set the gain at an optimum level, it has been shown [2] that if the gain is limited to, at most, the rate of rotation of  $\boldsymbol{\omega}_\perp$  with respect to the body-fixed frame, detumbling is achieved within a reasonable timescale. This causes the rate of change of  $\boldsymbol{\omega}_\perp$  due to the control torque to be proportional to the rate of change caused by the rotation rate of the Earth's magnetic field vector. The full derivation can be found in the literature [2]. A reasonable estimate for the gain of the Bdot controller is given by:

$$k_\omega = 2\Omega(1 + \sin \xi/m)\mathcal{I}_{min} \quad (5)$$

### 3.5 Angular Rate feedback

The form of the dynamic equation is:

$$\mathcal{I}\dot{\boldsymbol{\omega}} + \boldsymbol{\omega}^\times \mathcal{I}\boldsymbol{\omega} = \left( \mathbf{K} \boldsymbol{\omega}^\times \mathbf{B} \right)^\times \mathbf{B}(t) \quad (6)$$

Using a vector triple product identity, this can be rewritten as:

$$\mathcal{I}\dot{\boldsymbol{\omega}} + \boldsymbol{\omega}^\times \mathcal{I}\boldsymbol{\omega} = -\mathbf{K} \left( \mathbf{B}\mathbf{B}^T - (\mathbf{B}^T \mathbf{B})\mathbf{1} \right) \boldsymbol{\omega} = \mathbf{M}$$

Using the kinetic energy of the system as a Lyapunov function, we find:

$$\begin{aligned} V &= \frac{1}{2} \boldsymbol{\omega}^T \mathcal{I} \boldsymbol{\omega} \\ \dot{V} &= \boldsymbol{\omega}^T \mathbf{M} = -\boldsymbol{\omega}^T \mathbf{K} \left( \mathbf{B}\mathbf{B}^T - (\mathbf{B}^T \mathbf{B})\mathbf{1} \right) \boldsymbol{\omega} \end{aligned}$$

Clearly  $\dot{V}$  is only negative semidefinite, since  $\dot{V} \Rightarrow 0$  both when  $\boldsymbol{\omega} = 0$  as well as when  $\boldsymbol{\omega}$  lies in the same direction as  $\mathbf{B}$ . This is due to the fact that no torques can be produced in this situation to decrease the rotational kinetic energy of the system. A complete proof of asymptotic stability for the Lyapunov function presented above can be found in literature [2].

The maximum control torque that can be generated occurs when the dipole vector lies in a plane perpendicular to the Earth's magnetic field vector. We constrain the vectors  $\mathbf{m}$  and  $\mathbf{B}$  to be orthogonal to one another via:

$$\mathbf{m} = \hat{\mathbf{B}}^\times \mathbf{M} = \hat{\mathbf{B}}^\times \mathbf{K} \left( \mathbf{B}\mathbf{B}^T - (\mathbf{B}^T \mathbf{B})\mathbf{1} \right) \boldsymbol{\omega}$$

Only the directionality of the magnetic field matters in this form of  $\mathbf{m}$ , since we can divide by the magnitude of the magnetic field vector and the measured values can all be absorbed into the gain matrix  $\mathbf{K}$ . Thus, if rate measurements are available, along with the magnetic field measurements, we can maintain passivity by feeding back  $\mathbf{m}$  as shown above, where  $\mathbf{m}$  is now of the form:

$$\begin{aligned} \mathbf{m} &= \hat{\mathbf{B}}^\times \mathbf{K} \left( \hat{\mathbf{B}}\hat{\mathbf{B}}^T - \mathbf{1}_3 \right) \boldsymbol{\omega} \\ &= -\hat{\mathbf{B}}^\times \mathbf{K} \boldsymbol{\omega} \end{aligned}$$

By choosing the correct  $\mathbf{K}$  matrix, it can be shown that the gain matrix can be simplified into a scalar, resulting in a dipole moment of the form:

$$\mathbf{m} = -k_\omega \hat{\mathbf{B}}^\times \boldsymbol{\omega}$$

### 3.6 State feedback

While the previous section dealt with the feedback of angular rates, a full state feedback law can be introduced that drives both the angular velocity of the spacecraft to zero, and drives the attitude towards a specific value [7]. We will use this to compare the performance of our two controllers. Consider the form of the dynamic equation:

$$\mathcal{I}\dot{\boldsymbol{\omega}} + \boldsymbol{\omega}^\times \mathcal{I}\boldsymbol{\omega} = \boldsymbol{\tau} \quad (7)$$

We will now feedback the angular rate and attitude of the spacecraft, using a control law of the form:

$$\boldsymbol{\tau} = -\epsilon^2 k_p \mathbf{q} - \epsilon k_r \boldsymbol{\omega}$$

#### 3.6.1 Stability

The stability of this law has been demonstrated [6], however it is well beyond the scope of this course. The result is summarized below:

Consider the system:

$$\dot{\mathbf{q}} = \frac{1}{2} \boldsymbol{\omega} \mathbf{q} \quad , \quad \dot{\boldsymbol{\omega}} = \mathcal{I}^{-1} [\mathbf{u} - \boldsymbol{\omega}^\times \mathcal{I}\boldsymbol{\omega}]$$

With the control law:

$$\boldsymbol{\tau} = -(\epsilon^2 k_p \mathbf{q} + \epsilon k_r \boldsymbol{\omega})$$

And consider the equilibrium given by:

$$(\bar{\mathbf{q}}, \mathbf{0}) = \left( \begin{bmatrix} 0 \\ 0 \\ 0 \\ 1 \end{bmatrix}, \begin{bmatrix} 0 \\ 0 \\ 0 \end{bmatrix} \right)$$

There exists an  $\epsilon^* > 0$  such that for any  $0 < \epsilon < \epsilon^*$  the control law  $\boldsymbol{\tau}$  ensures that the equilibrium  $(\mathbf{q}, \mathbf{0})$  is a locally asymptotically stable equilibrium for the closed loop system described above.

### 3.7 Linearized Model

The general form of a linear, time variant (LTV) system, where small angles and rates have been assumed, can be expressed via:

$$\begin{aligned} \dot{\mathbf{x}}(t) &= \mathcal{A}(t)\mathbf{x}(t) + \mathcal{B}(t)\mathbf{u}(t) \\ \mathbf{y}(t) &= \mathcal{C}(t)\mathbf{x}(t) + \mathcal{D}(t)\mathbf{u}(t) \end{aligned}$$

To be able to linearize a nonlinear system an equilibrium must be chosen. An Earth pointing orientation is chosen, and the desired angular velocity and attitude states are defined as:

$$\boldsymbol{\omega} = [0 \quad -\Omega \quad 0]^T \quad , \quad \mathbf{q} = [0 \quad 0 \quad 0 \quad 1]^T$$

Where these desired states are describing the motion of the inertial frame with respect to the body fixed frame, as expressed in the body fixed frame. In other words, this desired state occurs when the transformation between the principal body fixed frame and the orbital body fixed frame is the identity matrix.

Any deviation of the principal body fixed frame from the orbital body fixed frame can be thought of as a perturbation to the system. The states around the equilibrium, and the subsequent state vector that will be used, are given by

$$\delta\boldsymbol{\omega} = \begin{bmatrix} \delta\omega_x \\ \delta\omega_y - \omega_0 \\ \delta\omega_z \end{bmatrix} \quad , \quad \delta\mathbf{q} = \begin{bmatrix} \delta\epsilon_1 \\ \delta\epsilon_2 \\ \delta\epsilon_3 \\ 1 \end{bmatrix} \quad , \quad \mathbf{x} = \begin{bmatrix} \delta\boldsymbol{\omega} \\ \delta\boldsymbol{\epsilon} \end{bmatrix} = [\delta\omega_x \quad \delta\omega_y \quad \delta\omega_z \quad \delta\epsilon_1 \quad \delta\epsilon_2 \quad \delta\epsilon_3]^T$$

Where the fourth Euler parameter has been neglected, since it can be defined in terms of the other three parameters, namely:

$$\eta = \sqrt{1 - \epsilon_1^2 + \epsilon_2^2 + \epsilon_3^2}$$

The kinematic differential equation can be written as:

$$\delta\dot{\boldsymbol{\varepsilon}} = \begin{bmatrix} \frac{1}{2} & 0 & 0 & 0 & 0 & \frac{1}{2}\omega_0 \\ 0 & \frac{1}{2} & 0 & 0 & 0 & 0 \\ 0 & 0 & \frac{1}{2} & -\frac{1}{2}\omega_0 & 0 & 0 \end{bmatrix} \begin{bmatrix} \delta\boldsymbol{\omega} \\ \delta\boldsymbol{\varepsilon} \end{bmatrix}$$

While the homogeneous dynamic differential equation can be written in terms of the disturbances as:

$$-\mathcal{I}^{-1}[\boldsymbol{\omega}^\times \mathcal{I}\boldsymbol{\omega}] \approx \begin{bmatrix} \frac{\mathcal{I}_y - \mathcal{I}_z}{\mathcal{I}_x} \omega_0 \delta\omega_z \\ 0 \\ \frac{\mathcal{I}_x - \mathcal{I}_y}{\mathcal{I}_z} \omega_0 \delta\omega_x \end{bmatrix} = \begin{bmatrix} k_x \omega_0 \delta\omega_z \\ 0 \\ k_z \omega_0 \delta\omega_x \end{bmatrix}$$

Where  $k_x = \frac{\mathcal{I}_y - \mathcal{I}_z}{\mathcal{I}_x}$ ,  $k_y = \frac{\mathcal{I}_z - \mathcal{I}_x}{\mathcal{I}_y}$  and  $k_z = \frac{\mathcal{I}_x - \mathcal{I}_y}{\mathcal{I}_z}$ . Note that due to this being a linearized model, higher order terms ( $\delta\omega_i \delta\omega_j \approx 0$ ) are neglected.

Gravity gradient torques can be represented by the following form:

$$\boldsymbol{\tau}_{gg} = \frac{3\mu}{r^5} \mathbf{r}^\times \mathcal{I} \mathbf{r}$$

Where  $\mathbf{r}$  is the position vector extending from the Earth's center to the position of the orbiting spacecraft. In order to transform this vector into the orbital frame we must use the third column of the transformation matrix, namely:

$$\begin{aligned} \mathbf{C}_{io} &= (\eta^2 - \boldsymbol{\varepsilon}^T \boldsymbol{\varepsilon}) \mathbf{1}_3 + 2\boldsymbol{\varepsilon} \boldsymbol{\varepsilon}^T - 2\eta \boldsymbol{\varepsilon}^\times \\ &= \begin{bmatrix} 1 - 2(\varepsilon_2^2 + \varepsilon_3^2) & 2(\varepsilon_1 \varepsilon_2 + \varepsilon_3 \eta) & 2(\varepsilon_1 \varepsilon_3 - \varepsilon_2 \eta) \\ 2(\varepsilon_1 \varepsilon_2 - \varepsilon_3 \eta) & 1 - 2(\varepsilon_1^2 + \varepsilon_3^2) & 2(\varepsilon_2 \varepsilon_3 + \varepsilon_1 \eta) \\ 2(\varepsilon_1 \varepsilon_3 + \varepsilon_2 \eta) & 2(\varepsilon_2 \varepsilon_3 - \varepsilon_1 \eta) & 1 - 2(\varepsilon_1^2 + \varepsilon_2^2) \end{bmatrix} \end{aligned}$$

Therefore,

$$\boldsymbol{\tau}_{gg} = 3 \frac{\mu}{r^3} \mathbf{C}_{io} \begin{bmatrix} 0 \\ 0 \\ 1 \end{bmatrix}^\times \mathcal{I} \mathbf{C}_{io} \begin{bmatrix} 0 \\ 0 \\ 1 \end{bmatrix} = 3\omega_0^2 \begin{bmatrix} 2(\varepsilon_1 \varepsilon_3 - \varepsilon_2 \eta) \\ 2(\varepsilon_2 \varepsilon_3 + \varepsilon_1 \eta) \\ 1 - 2(\varepsilon_1^2 + \varepsilon_2^2) \end{bmatrix}^\times \mathcal{I} \begin{bmatrix} 2(\varepsilon_1 \varepsilon_3 - \varepsilon_2 \eta) \\ 2(\varepsilon_2 \varepsilon_3 + \varepsilon_1 \eta) \\ 1 - 2(\varepsilon_1^2 + \varepsilon_2^2) \end{bmatrix}$$

Noting that, due to the disturbance torques we have been considering,  $\delta\varepsilon_i \cdot \delta\varepsilon_j \approx \delta\varepsilon_i^2 \approx 0$  for  $i, j = 1, 2, 3$ . Then, the linearized dynamics including the gravity gradient torques may be written:

$$\delta\dot{\boldsymbol{\omega}} = \begin{bmatrix} 0 & 0 & -k_x \omega_0 & -6k_x \omega_0^2 & 0 & 0 \\ 0 & 0 & 0 & 0 & 6k_y \omega_0^2 & 0 \\ -k_z \omega_0 & 0 & 0 & 0 & 0 & 0 \end{bmatrix} \begin{bmatrix} \delta\omega_x \\ \delta\omega_y \\ \delta\omega_z \\ \delta\varepsilon_1 \\ \delta\varepsilon_2 \\ \delta\varepsilon_3 \end{bmatrix} + \mathcal{I}^{-1} \boldsymbol{\tau}_{magnetic}$$

Combining this with our expression for the kinematic differential equation, we obtain our  $\mathcal{A}$  matrix:

$$\mathcal{A} = \begin{bmatrix} 0 & 0 & -k_x \omega_0 & -6k_x \omega_0^2 & 0 & 0 \\ 0 & 0 & 0 & 0 & 6k_y \omega_0^2 & 0 \\ -k_z \omega_0 & 0 & 0 & 0 & 0 & 0 \\ \frac{1}{2} & 0 & 0 & 0 & 0 & \frac{1}{2}\omega_0 \\ 0 & \frac{1}{2} & 0 & 0 & 0 & 0 \\ 0 & 0 & \frac{1}{2} & -\frac{1}{2}\omega_0 & 0 & 0 \end{bmatrix}$$

The system's  $\mathcal{B}$  matrix is already linear:

$$\boldsymbol{\tau}_{magnetic} = \mathbf{m}^\times \mathcal{B}$$

The magnetic dipoles on board can be made more efficient by including an extra cross term, so as to only create control torques that include moments which are perpendicular to the local magnetic field:

$$\begin{aligned} \boldsymbol{\tau}_{magnetic} &= (\mathbf{m}_\parallel + \mathbf{m}_\perp)^\times \mathcal{B} \\ \tilde{\mathbf{m}} &\mapsto \mathbf{m} : \mathbf{m} = \tilde{\mathbf{m}}^\times \mathcal{B} \\ \therefore \quad \boldsymbol{\tau}_{magnetic} &= \left( \frac{\mathbf{m}^\times \mathcal{B}}{|\mathcal{B}|} \right)^\times \mathcal{B} \end{aligned}$$



We can then use the triple cross product identity to rewrite the product as:

$$\boldsymbol{\tau}_{\text{magnetic}} = \left( \frac{\mathbf{B}\mathbf{B}^T - (\mathbf{B}^T\mathbf{B})\mathbf{1}_3}{|\mathbf{B}|} \right) \mathbf{m} = \mathbf{B}\mathbf{m}$$

Thus, the  $\mathbf{B}$  matrix is given by:

$$\mathbf{B} = \mathcal{I}^{-1} \begin{bmatrix} -(b_y^2 + b_z^2) & b_x b_y & b_x b_z \\ b_x b_y & -(b_x^2 + b_z^2) & b_y b_z \\ b_x b_z & b_y b_z & -(b_x^2 + b_y^2) \\ 0 & 0 & 0 \\ 0 & 0 & 0 \\ 0 & 0 & 0 \end{bmatrix}$$

The above form is a linear quadratic regulator problem (LQR). The optimal feedback of the linearized system presented above is determined by minimizing the performance index, which is given by:

$$\mathcal{J} = \frac{1}{2} \mathbf{x}^T(t_f) \mathbf{S} \mathbf{x}(t_f) + \frac{1}{2} \int_0^{t_f} [\mathbf{x}^T \mathbf{Q} \mathbf{x} + \mathbf{u}^T \mathbf{R} \mathbf{u}] dt$$

Where  $\mathbf{Q}$  and  $\mathbf{R}$  are assumed to be symmetric and positive definite. Due to the time varying nature of the Earth's magnetic field as seen by a spacecraft in orbit, two options have been investigated thoroughly.

The first option is to solve the periodic Riccati equation for a set of time varying, but periodic gains. In this way, the gains can be stored on board the satellite, and based on orbital position, the correct set of gains can be employed to control the spacecraft. Several issues arise with this method:

- The spacecraft will be subject to a number of different uncertainties, including unanticipated behavior of the Earth's magnetic field, variations in the disturbance torques experienced, and uncertainties in the spacecraft's moments of inertia.
- The controller is very sensitive to the periodic nature of the gain of the system. Any variations in the synchronization of the orbit result in a non-optimal gain scheme being applied to the spacecraft.
- Both secular and cyclic disturbance torques must be simultaneously attenuated, while the actuators are limited in the dipoles that can be produced due to saturation.

If a periodic control system is implemented, Floquet theory can be used to determine stability of the periodic state transition matrix.

The second option involves using constant gain feedback control. This method is far from ideal since the magnetic field is hardly constant. However, a gain scheme may be optimized for the average magnitude of the magnetic field vector throughout a single orbit. In this situation, the optimal feedback may be determined from the algebraic Riccati equation, namely:

$$\bar{\mathbf{P}}\mathbf{A} + \mathbf{A}^T \bar{\mathbf{P}} - \bar{\mathbf{P}}\mathbf{B}\mathbf{R}^{-1}\mathbf{B}^T \bar{\mathbf{P}} + \mathbf{Q} = 0$$

The optimal feedback is then given by:

$$\mathbf{u}(t) = -\mathbf{R}^{-1}\mathbf{B}^T \bar{\mathbf{P}}$$

Where the poles of the closed loop system may be place via apt choices of  $\mathbf{Q}$  and  $\mathbf{R}$  if the system is controllable, or if it is uncontrollable but the uncontrollable modes have stable eigenvalues.

## 4 Simulation

A model was developed in matlab in order to demonstrate the feasibility of the various control laws discussed above. A random number generator was used to determine the initial angular velocity vector  $\boldsymbol{\omega}$ , however every simulation used the same initial conditions. The initial attitude was set to  $\mathbf{q} = [0 \ 0 \ 0 \ 1]^T$ . The moments of inertia were chosen to be unsymmetrical, but close in value. Altitudes were varied between 150km and 1650km, but kept within low Earth orbit. Inclinations were varied from 0° to 90° with respect to Earth's equatorial plane. The fourth order Runge-Kutta Method was used to solve the differential equations (ODE4 package in matlab).

The complete matlab script can be found in the appendix.

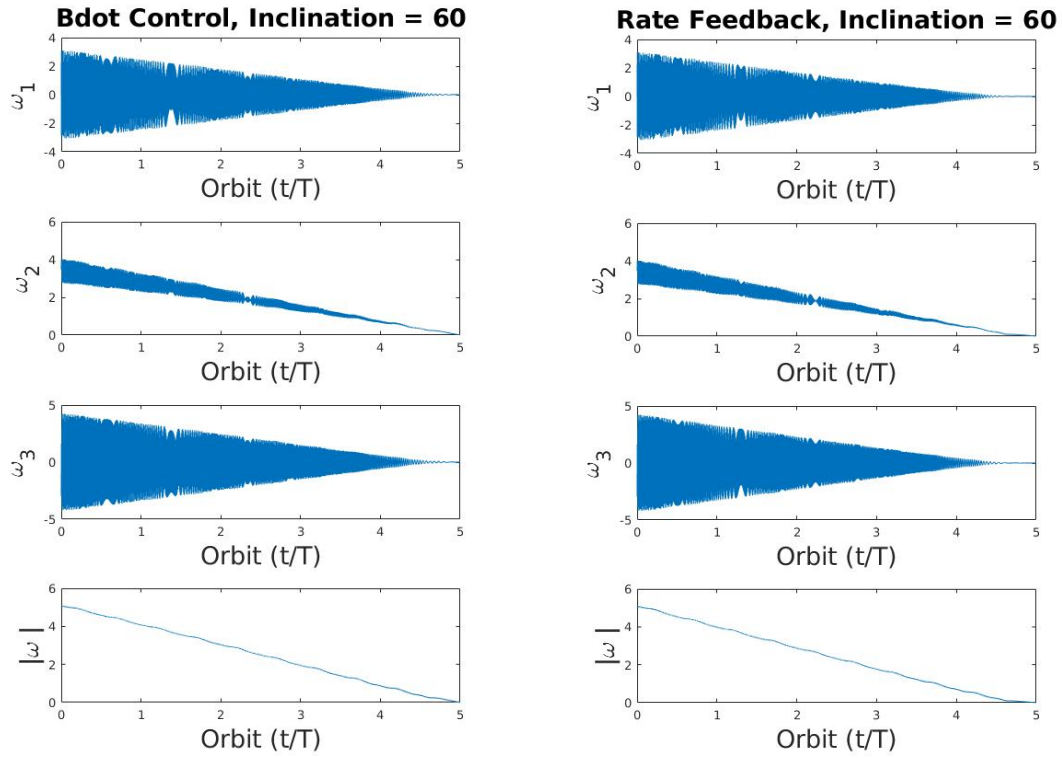


Figure 1: Comparison of Bdot control and rate feedback control at an altitude of 900km.

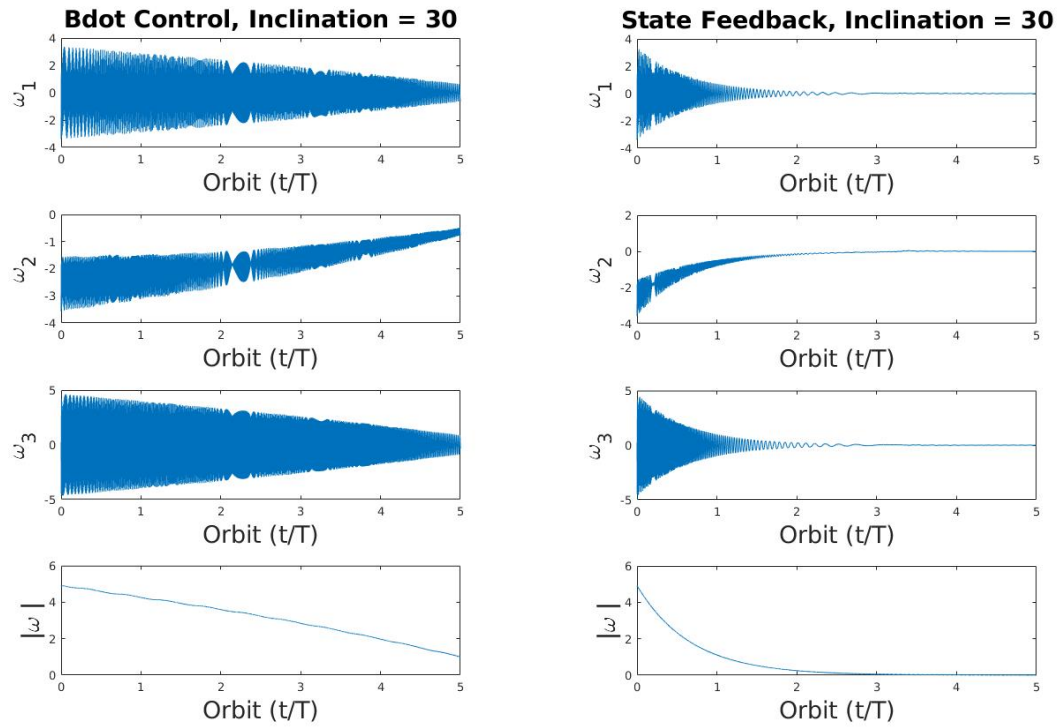


Figure 2: Comparison of Bdot control and full state feedback control at an altitude of 150km.

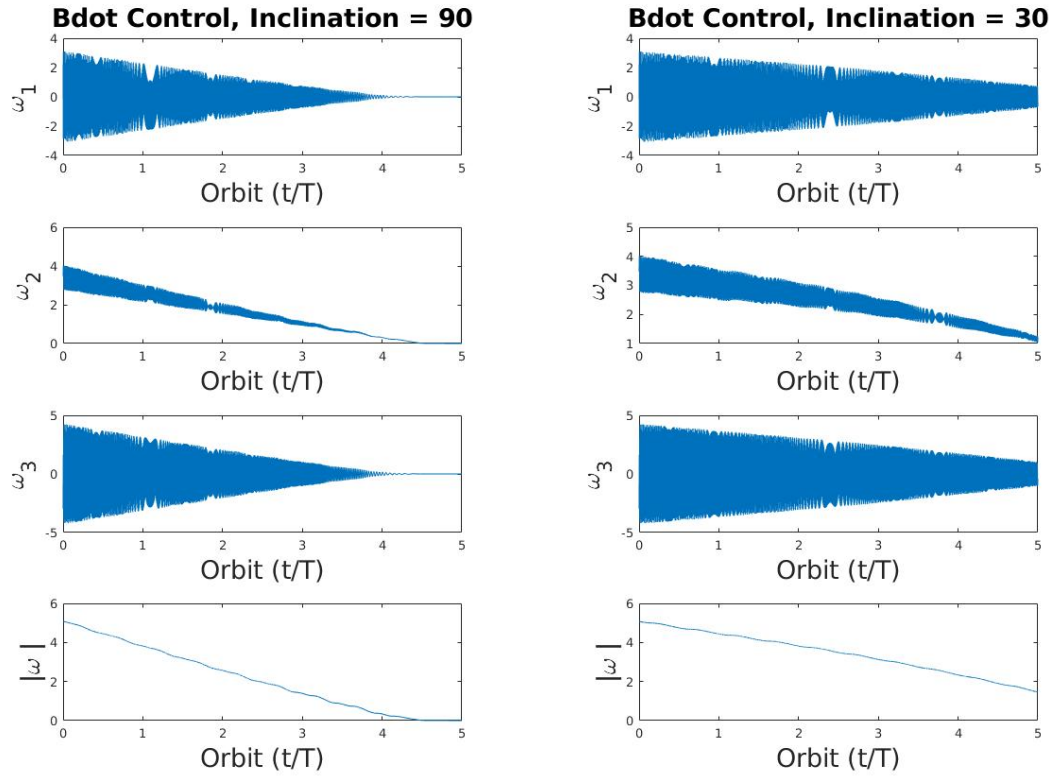
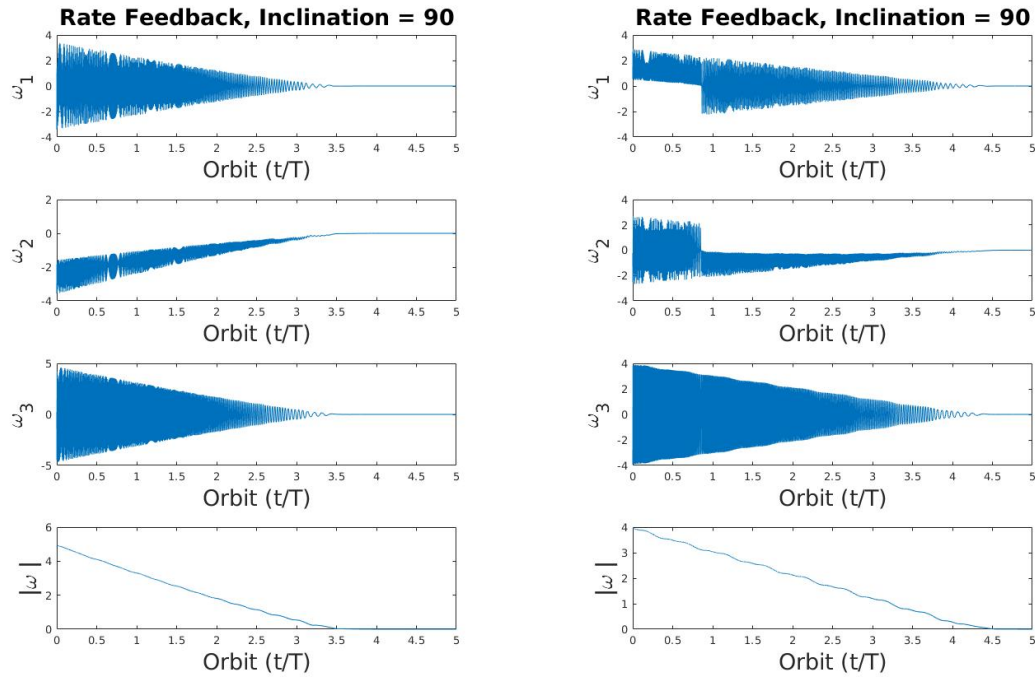


Figure 3: Comparison of Bdot control law at varying orbital inclinations, at an altitude of 900km



(a) Altitude = 150km

(b) Altitude = 1500km

Figure 4: Effect of altitude on time to reach steady state.

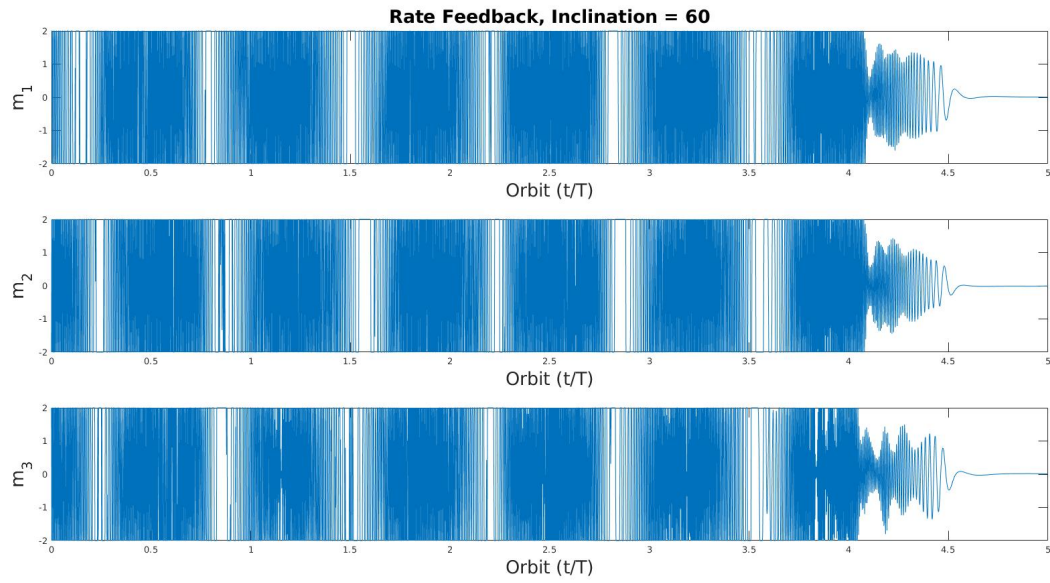


Figure 5: Bdot control magnetic dipole feedback value during detumble maneuver.

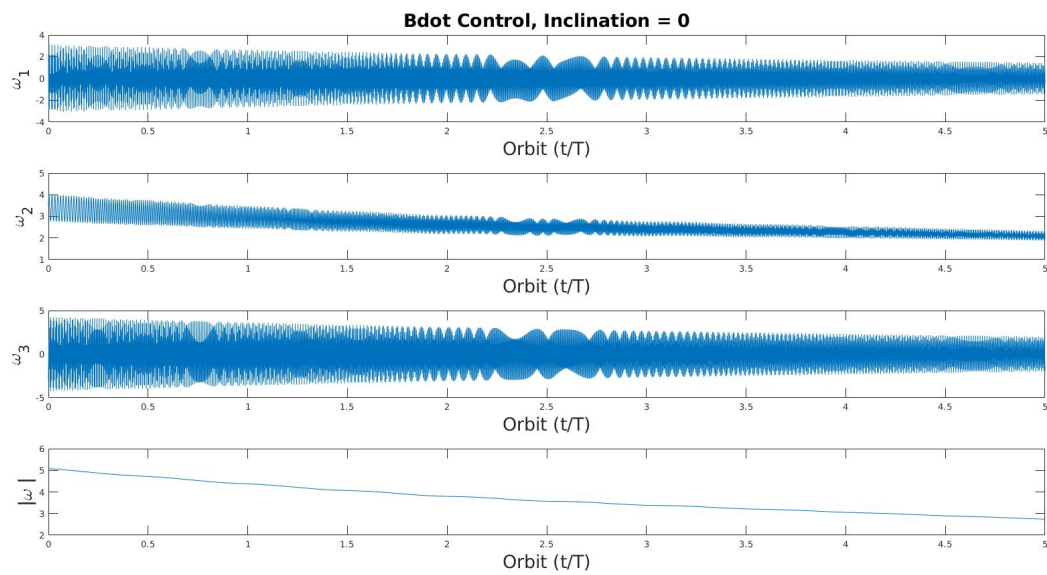


Figure 6: Bdot feedback control in near geomagnetic equatorial orbit.

## 5 Discussion

Figures 1 and 2 compare the effect of each control law on the magnetically actuated detumble maneuver. Note that, since the gain associated with the rate feedback law is chosen to be equivalent to the gain associated with the  $\dot{\mathbf{b}}$  feedback law, according to equation 5. Due to this similarity, along with their both being proportional to  $\omega$ , these two control laws exhibit very similar effects on the angular rates of the spacecraft, with almost identical times taken to reach steady state.

The state feedback law, though chosen to have a gain that is approximately equal to the gain chosen for the rate and  $\dot{\mathbf{b}}$  feedback laws, reaches steady state in a much more efficient manner. Figure 2 demonstrates the disadvantage of the underactuated nature of magnetically actuated control laws.

Figure 3 demonstrates a very important aspect of purely magnetically actuated control laws: when the direction of the magnetic field stays roughly constant (i.e the inclination of the orbital plane with respect to the Earth's geomagnetic equatorial plane is small), the control law encounters a much longer detumble time. When the Earth's magnetic field vector changes it's direction more significantly over an orbit, the control law is able to make use of all three dipole moments and reduce the angular velocity more efficiently.

Altitude also plays an important role in the time necessary for the magnetically actuated spacecraft to reach steady state. It should be noted that even though the orbital period of the spacecraft orbiting at an altitude of 1500km will be significantly longer than that of a spacecraft orbiting at an altitude 150km, figure 4 demonstrates that the difference in the Earth's magnetic field strength between those two altitudes is significant enough to still drive the spacecraft to a steady state in a shorter number of orbits. Thus, magnetic actuation becomes more efficient as the orbital radius of the spacecraft decreases, making magnetic actuation a more attractive candidate for low earth orbit missions.

The magnetic dipole moments in figure 5 provide two interesting insights: first, given the constraint on the maximum magnetic dipole that can be generated by the magnetic torquers, the control drives the electromagnetic coils to saturation for  $\frac{4}{5}$  of the detumble maneuver; clearly more powerful electromagnets are required to detumble the spacecraft more efficiently. Second, it can be seen that there are sections where no dipole moment is generated. It can be inferred that this is due to the way the rate feedback law was developed: when the magnetic dipole is aligned with the Earth's magnetic field vector, the orthogonality of the feedback law with the Earth's magnetic field prevents the magnetic torquer from generating a magnetic moment, thus conserving the electricity that would otherwise be wasted.

Finally, figure 6 demonstrates the fatal flaw of purely magnetically actuated control systems. As was hinted at in 3, the closer the orbital plane is to coinciding with the Earth's geomagnetic equatorial plane, the longer the detumble maneuver will take, due to futility of attempting to generate a torque in the direction of the magnetic field vector. While angular velocity is still decreasing, it is doing so at a much slower rate, reducing the viable candidacy for this type of control law on missions that have low inclination orbits.

## 6 Conclusion

Several control laws were investigated via simulation to determine their effectiveness in detumbling spacecraft in low earth orbit. The standard  $\dot{\mathbf{b}}$  control law, as well as the rate feedback control law, were found to be especially useful for high inclination, low altitude orbits.

A linearized model was developed, however the optimal control determined by the algebraic Riccati equation was not effective in detumbling the spacecraft in this highly non-linear dynamical problem. The form of the linearized equations would allow for the development of a Linear time-periodic solution, which would be the next step in the development of this paper. Additional exploration would be directed towards a PD or PI control law, so that attitude and other states could be incorporated in the closed loop feedback.

Further investigation should be directed towards using magnetic actuation in tandem with other types of attitude control. Independently, the underactuated nature of magnetic attitude control severely restricts the situations in which it can be used. However, its reliability, low weight, and lack of need for propellant makes this form of attitude control an excellent candidate for support roles in spacecraft attitude control.

## References

- [1] A. Astolfi and M. Lovera. “Global spacecraft attitude control using magnetic actuators”. In: *Proceedings of the 2002 American Control Conference (IEEE Cat. No.CH37301)* (2002), pp. 1331–1335. DOI: 10.1109/acc.2002.1023205.
- [2] Giulio Avanzini and Fabrizio Giuliotti. “Magnetic Detumbling of a Rigid Spacecraft”. In: *Journal of Guidance, Control, and Dynamics* 35.4 (2012), pp. 1326–1334. DOI: 10.2514/1.53074.
- [3] S.p. Bhat and A.s. Dham. “Controllability of spacecraft attitude under magnetic actuation”. In: *42nd IEEE International Conference on Decision and Control (IEEE Cat. No.03CH37475)* (2003). DOI: 10.1109/cdc.2003.1272976.
- [4] Hari B. Hablani. “Comparative stability analysis and performance of magnetic controllers for bias momentum satellites”. In: *Journal of Guidance, Control, and Dynamics* 18.6 (1995), pp. 1313–1320. DOI: 10.2514/3.21547.
- [5] M. Lovera, E. De Marchi, and S. Bittanti. “Periodic attitude control techniques for small satellites with magnetic actuators”. In: *IEEE Transactions on Control Systems Technology* 10.1 (2002), pp. 90–95. DOI: 10.1109/87.974341.
- [6] Marco Lovera and Alessandro Astolfi. “Global Magnetic Attitude Control of Inertially Pointing Spacecraft”. In: *Journal of Guidance, Control, and Dynamics* 28.5 (2005), pp. 1065–1072.
- [7] Marco Lovera and Alessandro Astolfi. “Global Spacecraft Attitude Control Using Magnetic Actuators”. In: *Advances in Dynamics and Control* (2004), pp. 1405–1414. DOI: 10.1201/9780203298916.ch1.
- [8] F. Martel, P.Pal, and M.Psiaki. “Active magnetic control system for gravity gradient stabilized spacecraft”. In: *Proceedings of the 2nd Annual AIAA/USU Conference on Small Satellites* ().
- [9] K.L. Musser and L.E. Ward. *Autonomous spacecraft attitude control using magnetic torquing only*. Tech. rep. 1989.
- [10] Mark Psiaki. “Magnetic torquer attitude control via asymptotic periodic linear quadratic regulation”. In: *AIAA Guidance, Navigation, and Control Conference and Exhibit* (2000). DOI: 10.2514/6.2000-4043.
- [11] Enrico Silani and Marco Lovera. “Magnetic spacecraft attitude control: a survey and some new results”. In: *Control Engineering Practice* 13.3 (2005), pp. 357–371. DOI: 10.1016/j.conengprac.2003.12.017.
- [12] A. Stickler and K. Alfrend. “An elementary magnetic attitude control system”. In: *Mechanics and Control of Flight Conference* (May 1974). DOI: 10.2514/6.1974-923.
- [13] Ping Wang and Yuri Shtessel. “Satellite Attitude Control Via Magnetorquers Using Switching Control Laws”. In: *IFAC Proceedings Volumes* 32.2 (1999), pp. 8021–8026. DOI: 10.1016/s1474-6670(17)57368-1.
- [14] J.t.-Y. Wen and K. Kreutz-Delgado. “The attitude control problem”. In: *IEEE Transactions on Automatic Control* 36.10 (1991), pp. 1148–1162. DOI: 10.1109/9.90228.
- [15] James P. Wertz. *Spacecraft attitude determination and control*. Kluwer, 1978.
- [16] John S. White, Fred H Shigemoto, and Kent Bourquin. *Satellite attitude control utilizing the earth’s magnetic field*. Tech. rep. Ames Research Center, Moffett Field, California, Aug. 1961.
- [17] Rafal Wisniewski. “Linear Time-Varying Approach to Satellite Attitude Control Using Only Electromagnetic Actuation”. In: *Journal of Guidance, Control, and Dynamics* 23.4 (2000), pp. 640–647. DOI: 10.2514/2.4609.
- [18] Rafal Wisniewski and Rafal Wisniewski. “Linear time varying approach to satellite attitude control using only electromagnetic actuation”. In: *Guidance, Navigation, and Control Conference* (Nov. 1997). DOI: 10.2514/6.1997-3479.
- [19] Mark Wood, Wen-Hua Chen, and Denis Fertin. “Model Predictive Control of Low Earth Orbiting Spacecraft with Magneto-torquers”. In: *2006 IEEE International Conference on Control Applications* (2006). DOI: 10.1109/cca.2006.286071.
- [20] Andrea Maria Zanchettin, Alberto Calloni, and Marco Lovera. “Robust Magnetic Attitude Control of Satellites”. In: *IEEE/ASME Transactions on Mechatronics* 18.4 (2013), pp. 1259–1268. DOI: 10.1109/tmech.2013.2259843.

## 7 Matlab Code

```

1  close all
2  clear all
3  clc
4
5  % Parameters for Simulation
6
7  numeroforbits = 5;
8  SCInertia = diag([0.33,0.37,0.35]); % kg/m^2
9  MaxDipoleMoment = 2.0; % A*m^2
10 EarthMagMoment = 7.8379*10^6; % T*km^3
11 GeoTiltAngle = 11.44*pi/180; % rad
12 EarthRotation = 7.292116*10^(-5); % rad/s
13 SampleTime = 10; % s
14 StepTime = 0.1; % s
15 inclinationarray = linspace(0,90,4);
16 Altitudearray = linspace(6521,8021,3);
17
18 NumSims = length(Altitudearray)*length(inclinationarray);
19 SimsLeft = NumSims
20
21 % Main Program Loop
22 for i =1:length(Altitudearray)
23     % Initial Conditions
24     r = -4 + (8).*rand(3,1);
25     q0 = [ 0; 0; 0; 1];
26     Omega0 = [ r(1); r(2); r(3) ];
27     for j = 1:length(inclinationarray)
28
29         % Relevant parameters for iteration
30         Rorbit = Altitudearray(i); %km
31         Inclination = inclinationarray(j)*pi/180; % rad
32         Torbit = 2*pi*sqrt(((Rorbit*1000)^3)/(3.986*10^14)); % s
33         SimTime = numeroforbits*Torbit; % s
34         DipoleMag = EarthMagMoment / Rorbit^3; % T
35         OrbitalSpeed = 2*pi/Torbit; % rad/s
36         TotalTime = zeros(round(SimTime/SampleTime)+1,1);
37
38         % Bdot Gain Calculation
39         Beta1 = 0;
40         CosZeta = cos(Inclination)*cos(GeoTiltAngle) + sin(Inclination)*sin(
41             GeoTiltAngle)*cos(Beta1);
42         XI = atan2(-sin(GeoTiltAngle)*sin(Beta1), sin(Inclination)*cos(
43             GeoTiltAngle) - cos(Inclination)*sin(GeoTiltAngle)*cos(Beta1));
44         if sin(XI) ==0
45             SinZeta = sin(Inclination)*cos(GeoTiltAngle)-cos(Inclination)*sin(
46                 GeoTiltAngle)*cos(Beta1) / cos(XI);
47         else
48             SinZeta = -sin(GeoTiltAngle)*sin(Beta1)/sin(XI);
49         end
50         BdotGain = 2 * OrbitalSpeed * (1+SinZeta)*min(diag(SCInertia));
51
52         % Generate state vectors
53         YtBdot = [q0' Omega0' zeros(1,3); zeros(round(SimTime/SampleTime),10) ];
54         YtRate = [q0' Omega0' zeros(1,3); zeros(round(SimTime/SampleTime),10) ];
55         YtState = [q0' Omega0' zeros(1,3); zeros(round(SimTime/SampleTime),10) ];
56
57         % Solve Differential Equations
58         for k=1:round(SimTime/SampleTime) ,
59             YsBdot = ode4(@(t,Y) AttitudeDynamics(t,Y, Inclination , OrbitalSpeed ,

```

```

        EarthRotation , DipoleMag , GeoTiltAngle , SCInertia , MaxDipoleMoment ,
        BdotGain , StepTime , 1 , k) , ...
57     TotalTime(k) : StepTime : ( TotalTime(k)+SampleTime) , YtBdot(k,:) ');
58     YtBdot(k+1,:) = YsBdot(end,:);
59     YsRate = ode4(@(t,Y) AttitudeDynamics(t,Y, Inclination , OrbitalSpeed ,
        EarthRotation , DipoleMag , GeoTiltAngle , SCInertia , MaxDipoleMoment ,
        BdotGain , StepTime , 2 , k) , ...
60     TotalTime(k) : StepTime : ( TotalTime(k)+SampleTime) , YtRate(k,:) ');
61     YtRate(k+1,:) = YsRate(end,:);
62     YsState = ode4(@(t,Y) AttitudeDynamics(t,Y, Inclination , OrbitalSpeed ,
        EarthRotation , DipoleMag , GeoTiltAngle , SCInertia , MaxDipoleMoment ,
        BdotGain , StepTime , 3 , k) , ...
63     TotalTime(k) : StepTime : ( TotalTime(k)+SampleTime) , YtState(k,:) ');
64     YtState(k+1,:) = YsState(end,:);
65     TotalTime(k+1) = TotalTime(k)+SampleTime;
66     end
67
68     Bdot = sprintf( '%s_%d_%d.dat' , 'Bdot' , i , j );
69     Rate = sprintf( '%s_%d_%d.dat' , 'Rate' , i , j );
70     State = sprintf( '%s_%d_%d.dat' , 'State' , i , j );
71
72     mout(end+1,:) = mout(end,:);
73
74     BdotM = [ YtBdot mout(:,1:3) ];
75     RateM = [ YtRate mout(:,4:6) ];
76     StateM = [ YtState mout(:,7:9) ];
77
78     csvwrite(Bdot,BdotM)
79     csvwrite(Rate,RateM)
80     csvwrite(State,StateM)
81
82     SimsLeft = SimsLeft - 1
83
84     end
85 end
86
87 13
88
89 %% Functions
90
91 % Attitude Dynamic Model
92 function dydt = AttitudeDynamics(t,Y, Inclination , OrbitalSpeed , EarthRotation ,
    DipoleMag , GeoTiltAngle , SCInertia , MaxDipoleMoment , BdotGain , StepTime ,
    ControlScheme , k)
93     OrbitBodyAttTransform = (quat2dcm([Y(4) Y(1:3)']));
94     Beta1 = EarthRotation*t;
95     b = OrbitBodyAttTransform * MagneticField(OrbitalSpeed*t, Inclination ,
        GeoTiltAngle , Beta1 , DipoleMag);
96     Omegar = Y(5:7)-OrbitBodyAttTransform*[0;-OrbitalSpeed;0];
97     dydt(1:3,1) = (1/2)*(Y(4)*Omegar - cross(Omegar,Y(1:3)));
98     dydt(4,1) = -(1/2)*Omegar'*Y(1:3);
99     Bdot = (b-Y(8:10,1))/StepTime;
100    dydt(8:10,1) = Bdot;
101    % Chose Control Scheme
102    if ControlScheme == 1
103        ControlLaw = BdotControl(BdotGain/norm(b)^2,Bdot);
104    elseif ControlScheme == 2
105        ControlLaw = RateFeedbackControl(BdotGain/norm(b)^2,b,Y);
106    elseif ControlScheme == 3
107        ControlLaw = StateFeedbackControl(Y);
108    end

```



```

109 % Restrict dipole coils to saturation limit
110 for j=1:length(ControlLaw)
111     if abs(ControlLaw(j))>MaxDipoleMoment
112         ControlLaw(j)=sign(ControlLaw(j))*MaxDipoleMoment;
113     end
114 end
115 if ControlScheme == 3
116     dydt(5:7,1) = mldivide(SCInertia,(ControlLaw-cross(Y(5:7),SCInertia*Y
117         (5:7))));
118 else
119     dydt(5:7,1) = mldivide(SCInertia,(cross(ControlLaw,b)-cross(Y(5:7),
120         SCInertia*Y(5:7))));
121 end
122 % Record dipole moments
123 persistent m
124 if mod(floor(t),10) == 0
125     a = (ControlScheme-1)*3 + 1;
126     c = ControlScheme*3;
127     m(k,a:c) = ControlLaw;
128     assignin('base','mout',m)
129 end
130 end
131 function u=BdotControl(BdotGain,Bdot)
132     u = -BdotGain*Bdot;
133 end
134
135 function u=RateFeedbackControl(BdotGain,b,Y)
136     u = -(BdotGain*cross(b,Y(5:7)));
137 end
138
139 function u=StateFeedbackControl(Y)
140     u = -0.0001*Y(5:7) - 0.0001*Y(1:3);
141 end
142
143 function b=MagneticField(OrbitalSpeedTime,Inclination,GeoTiltAngle,Beta1,
144     DipoleMag)
145     CosZeta = cos(Inclination)*cos(GeoTiltAngle) + sin(Inclination)*sin(
146         GeoTiltAngle)*cos(Beta1);
147     XI = atan2(-sin(GeoTiltAngle)*sin(Beta1),sin(Inclination)*cos(GeoTiltAngle)
148         - cos(Inclination)*sin(GeoTiltAngle)*cos(Beta1));
149     if sin(XI) ==0
150         SinZeta = sin(Inclination)*cos(GeoTiltAngle)-cos(Inclination)*sin(
151             GeoTiltAngle)*cos(Beta1) / cos(XI);
152     else
153         SinZeta = -sin(GeoTiltAngle)*sin(Beta1)/sin(XI);
154     end
155     b = DipoleMag * [SinZeta*cos(OrbitalSpeedTime - XI); -CosZeta; 2*SinZeta*sin
156         (OrbitalSpeedTime - XI)];
157 end

```